We are IntechOpen, the world's leading publisher of Open Access books Built by scientists, for scientists

4,800
Open access books available

122,000
International authors and editors

135M
Downloads

Our authors are among the

154
Countries delivered to

TOP 1%
most cited scientists

12.2%
Contributors from top 500 universities

CLARIVATE ANALYTICS BOOK CITATION INDEX INDEXED

WEB OF SCIENCE™

Selection of our books indexed in the Book Citation Index in Web of Science™ Core Collection (BKCI)

Interested in publishing with us?
Contact book.department@intechopen.com

Numbers displayed above are based on latest data collected.
For more information visit www.intechopen.com

Chapter 12

Submarine Volcanism of the Cabo de Gata Magmatic Arc in the Betic-Rif Orogen, SE Spain: Processes and Products

Carles Soriano, Ray A.F. Cas, Nancy R. Riggs and Guido Giordano

Additional information is available at the end of the chapter

http://dx.doi.org/10.5772/63579

Abstract

Volcanic eruptions in subaqueous settings have been traditionally characterized by the study of ancient deposits and, more recently, by indirect observation of the sea floor with different geophysical means. Subaqueous volcanism is largely governed by the physical properties of water and the way water interacts with magma. Among the characteristic products of subaqueous volcanism are hyaloclastite breccias of dense clasts and of pumiceous clasts produced by the quench fragmentation of hot magma in effusive eruptions. Pumice breccias driven by fragmentation of magma in explosive eruptions are not infrequent. The Miocene volcanic zone of Cabo de Gata in southeastern Spain provides excellent exposures where to test the current understanding on subaqueous volcanism. In particular, submarine lavas with a coherent core and an outer carapace of vesicular hyaloclastite together with pumice breccias and crystal tuffs of the El Barronal Formation provide clues to understand transient conditions during explosive and effusive eruptions. Debris avalanches deposits are rather common in Cabo de Gata, such as those of the Los Frailes Formation and the Cerro Estorvillas Formation, and help to understand the instability processes of submarine volcanic edifices and the resultant mass flows. Interbedding of volcanic rocks with shallow water sedimentary rocks allows inferring water depth conditions for volcanism and the subsidence history of the volcano-sedimentary basin.

Keywords: hyaloclastite, submarine explosions, debris-avalanche, subsidence, infralittoral

1. Introduction

The Cabo de Gata volcanic zone is located in southeastern Spain and is a portion of the Neogene volcanic arc of the Betic-rif Orogen, an arcuate orocline formed by westward retreat of an east

dipping slab Orogen, (**Figure 1**). The zone includes a wide variety of volcanic facies, ranging from explosive to effusive and recording transient conditions during eruptions. Volcanic rocks of Cabo de Gata are calc-alkaline in composition and were erupted from submarine vents and deposited in submarine settings, although rare facies record the transition to subaerial settings. Therefore, volcanism in Cabo de Gata is essentially submarine, although some volcanic edifices and products may have risen from above sea level. In terms of rock chemistry, eruptive style, age and depositional setting, volcanic successions in Cabo de Gata can be compared with similar examples from the volcanic arc of Japan. The Cabo de Gata volcanic zone constitutes the best exposed, best preserved and most voluminous record of the volcanic arc of the Betic-Rif Orogen and is certainly the most important record of submarine volcanism in the western Mediterranean area.

Despite its significance, it has not been until very recently that systematic studies with a modern facies to processes approach were undertaken in the Cabo de Gata volcanic zone and for this reason this area has remain virtually unknown for most volcanologists. Previous studies were mainly focused on petrological aspects of the volcanic rocks and on the Rodalquilar gold epithermal deposits associated with volcanic rocks, without providing a comprehensive stratigraphic framework aimed to understand the processes and products of Cabo de Gata volcanism [1–6]. Comparison of Cabo de Gata volcanic rocks with other Miocene volcanic zones such as the Iblean Mountains in Sicily, Sulcis in Sardegna and volcanic islands in the Aegean Sea may provide a more comprehensive view on volcanism of similar age occurring in different geotectonic scenarios of the narrow Mediterranean area.

Here, we first present an introductory section on the principles of subaqueous volcanism and then a review of our research undertaken during the last five years in the Cabo de Gata volcanic zone. In particular, we focus on those facies and successions of facies that reveal transient conditions of eruptive styles during eruptions and on submarine volcanic debris-avalanche deposits, which constitute a unique opportunity for a direct study of this kind of deposits in the geological record. We also focus on the facies and the stratigraphic successions of sedimentary rocks interbedded with volcanic rocks, aiming to characterize the bathymetric conditions for sediment deposition and, indirectly, for volcanism. Using the evidence provided by facies analyses we typify the characteristic eruptive models in Cabo de Gata and their link to the tectonics of the Neogene volcano-sedimentary basin in which volcanic rocks are exposed.

2. Basic principles of subaqueous volcanism

Understanding volcanic processes in subaqueous environments has always been challenging because first, in most cases, they cannot be directly observed, and second the physical properties of water and the way that water interacts with erupting or intruding magma are still not fully understood. Despite many contributions to the subject, the major debate still seems to revolve around the factors that relate water depths and explosive eruptions.

In modern environments, one of the greatest limitations has been the inability to observe processes and seafloor volcanic topography as well as the distribution of different facies or

http://dx.doi.org/10.5772/63579

deposit types at scales that provide understanding of the characteristics, extent, scale and relations of processes and deposits. Local submersible and camera observations have been helpful, but are very limiting. However, recent advances in imaging technology, such as high-resolution side-scan sonar and bathymetry technology mounted on autonomous underwater vehicles (AUVs) such as Sentry, allow very high-resolution Digital Elevation Model imagery to be produced over large areas and whole submerged volcanoes that will open up a new world of understanding of subaqueous volcanic processes. In addition, new generation photographic videoing and sampling facilities on remotely operated vehicles (ROVs) such as Jason and Medea provided hitherto unparalleled opportunities to learn about modern sea floor processes, including volcanism.

In ancient volcanic successions, the principal approach for understanding volcanological processes and settings remains detailed mapping of the relations between facies and analysis of their characteristics to assess original water depths and the process origins of the facies. This has given rise to an ongoing need to quantify the physical processes associated with subaqueous eruptions, including the constraints on processes imposed by subaqueous environments, in order to understand the origins of different deposit types.

The most recent review of submarine volcanic processes has been by [7] (see for a listing of other reviews and major research contributions) in which they provided a summary of the essential physical properties of water and magma, as well as a conceptual overview of the processes and deposit characteristics. To illustrate the concepts, they cited examples from the Cabo de Gata volcanic succession that has been well described by [8–12] and is summarized below in this paper. Recently, [13] quantified many of the physical processes involved in the formation of volcanic glass and the quench fragmentation of volcanic glass in subaqueous settings based on the materials-science literature. These authors then related the characteristics of hyaloclastite deposits to those physical processes and rates of processes. In this section, we briefly review the main processes, principles and deposit types in subaqueous environments.

The major difference between subaerial volcanism and subaqueous volcanism is the aqueous medium in the latter and the different ways that magma and water can interact to influence the style of eruption and the types of deposits. Water has a significant impact on the cooling rates of magma that is erupted into it, as well as creating ambient confining-pressure constraints on the way that exsolving magmatic volatiles and superheated water behave. Water is a high-enthalpy substance. It has a high heat capacity (4.187 kJ/kg K) and high thermal conductivity (0.58 W/m Kelvin at 25°C for water and 0.61 W/mK at 25°C, and 0.68 W/mK at 120°C for seawater [14]). Water is therefore very thermodynamically responsive to changes in temperature, which allow it to readily absorb and release heat transmitted to it by magma, via conduction and radiative-heat transfer. This is particularly important when magma at temperatures from 700 to 1200°C comes into contact with liquid water (<20°C). Water acts as a heat sink and can cause the magma to instantaneously cool through the glass transition temperature, causing glass to form. If the rate of heat loss or cooling rate is high, the magma/glass is thermally shocked, causing contractional tensile stresses to form in the glass. If these exceed the tensile strength of the glass, it shatters in situ, leading to a formation of a network of contractional fractures that propagate inwards from the cooling margin of the magma body.

This process is called quench fragmentation and the breccia of glass debris that forms is called hyaloclastite [7, 13]. This process can occur at any water depth.

However, water can very quickly change state over a limited temperature range (0–100°C) when superheated by contact with magma (700–1200°C) and over a range of external pressures that are determined by water depth. The hydrostatic pressure gradient in a body of water is 1 bar (0.1 MPa)/10 m water depth. In particular, liquid water can readily transform into steam, which has a much lower thermal conductivity (0.016 W/m K at 125°C) and specific heat capacity (1.996 kJ/kg K [15]). If this occurs at the interface between magma and water in a process called film boiling (also known as the Leidenfrost Effect), a vapour film forms at the interface, which can insulate the magma from heat loss. Sustained and efficient film boiling can thus reduce the rate of heat loss or cooling of the magma, moderate the rate of contraction, and so minimize thermal tensile stresses in the cooling glass. As a result, the magma may remain coherent and be preserved as a coherent lava or a coherent intrusion in the case where magma intrudes water-saturated sediments.

The super-heating of liquid water at low confining pressures causes a phase transformation to steam and a consequent major volume expansion. At high, instantaneous, rates of expansion such transformations are explosive, driving phreatic and phreatomagmatic volcanic explosions. This is most likely to occur at shallow water depths up to several hundred metres [16].

However, at increasing water depths and hydrostatic pressures the hydrostatic pressure approaches the critical pressure of water. The critical point of water is the pressure (and temperature) at which there is no distinction between the liquid and the gaseous phases; the fluid is called a supercritical fluid and has the properties of both the gaseous and the liquid forms. For pure water, the critical pressure is ~218–221 bars or 21.8–22.1 MPa and for seawater, it is about 300 bars or 30 MPa [17]. Since the hydrostatic pressure gradient in water is 1 bar or 0.1 MPa/10 m water depths, at water depths of 2 or more kms steam that forms at the interface between magma and the water mass is highly compressed and cannot expand explosively unless it can be instantaneously decompressed, which is difficult to do at those water depths. The modern seafloor record and the geological record tell us that voluminous explosive eruptions (cf. subaerial plinian eruptions) that occurred at water depths of more than 1 km are rare, although there are many examples of deposits of variably vesiculated pumiceous debris that originated in shallower water but were then resedimented into deeper water by various processes.

On this point, however, it is important to stress that not all pumice is explosive in origin. Coherent pumice domains can be well developed in subaerial lavas, formed through slow volatile exsolution and vesicle growth at nonexplosive rates in lavas with a subcritical volatile content to drive explosive eruption. In relatively deep subaqueous environments, the hydrostatic confining pressure will hinder both the initial exsolution of volatiles and the vesicle-growth rates. Growth rates may, however, be high enough to form well-vesiculated lavas with coherent pumice domains, but not high enough to drive explosions [7, 13]. Quench fragmentation of such coherent pumice domains can produce large volumes of pumice hyaloclastite.

http://dx.doi.org/10.5772/63579

Another factor that suppresses the intensity of submarine explosive eruptions is the bulk modulus of water, which for pure water is 2.15 × 109 Pa and for seawater is 2.34 × 109 Pa. The bulk modulus of a fluid is a measure of its resistance to uniform compression, i.e., its compressibility or the degree to which it deforms. In comparison, the adiabatic bulk modulus of air is orders of magnitude less, at 1.42 × 105 Pa. Because water is much less compressible and deformable than air, explosions into water are much more suppressed, restricted and much less intense than in air [7].

We now focus on the principal findings of [13] about the principles involved in the fracture behavior of volcanic glass, based on assessment of the ceramics and glass literature in materials science.

- Cooling contraction cracks propagate perpendicular to the cooling surfaces, which initially are the margins of the magma body at its interface with water or water-saturated sediments.
- The distance between cooling cracks depends on the cooling rate, the temperature differential and gradient between magma and water and the level of thermal stress. This determines the first-order grain size of the resultant hyaloclastite breccia and explains why grain size is smaller at the margins of a magma body compared with the interior, where cooling rates and temperature gradients are lower.
- Once a cooling crack forms, it also becomes a cooling surface and other cracks will form perpendicular to it and then others perpendicular to the second-order fractures, etc.
- The spacing between propagating cracks is usually equal to the length of the crack.
- When a crack approaches another crack, it will try to change direction and approach at right angles.
- When a crack intersects another crack, it will usually stop because it cannot propagate across the space.
- Crack formation results in release of both thermal and mechanical energy and cracks may stop if the tensile stress falls below the strength of the glass, which increases as glass cools.
- Crack shape, and thus fragment shape, depends on cooling rate, the crack propagation velocities and the orientation of the cooling surfaces. At high crack velocities, which occur when the temperature differential is high, cracks tend to be straight and form under what is called the critical crack regime. Crack velocities can be >600 ms^{-1}. At crack velocities greater than 0.25 times the speed of sound in glass, cracks may bifurcate and form wedge to splinter-shaped fragments. Low-temperature differentials lead to low crack velocities (subcritical regime (<cm s^{-1}) and cracks may become curviplanar.
- Water not only plays a physical role in facilitating crack propagation by causing cooling contraction tensile stresses at the crack tip but also plays a chemical role in breaking chemical bonds in the glass in a propagating crack tip.
- Heterogeneous glass, with dispersed crystals, lithic fragments and vesicles, experiences complex fracture formation because of the variable properties of the various components of the glass.

- Glass with abundant dispersed crystals is stronger than aphyric glass, is more resistant to quench fragmentation and, should it fragment, it is likely to form coarse hyaloclastite breccia.
- The presence of abundant vesicles in glass weakens it and makes it more prone to quench fragmentation.
- Pumice hyaloclastite formed through nonexplosive quench fragmentation should be quite common in submarine settings. If the deposit is still in situ, it may still preserve jigsaw fit textures. However, if it is resedimented, it should be bedded and preserve characteristics of a variety of subaqueous mass flow processes (e.g., grain-flow, turbidity currents, debris flow, debris avalanches and rafted suspension transport).

These principles and processes help to explain many of the characteristics of quench-fragmented hyaloclastite deposits, as described above, but also including the following:

- Equant, blocky clast aggregates are likely to have formed under steady, slow, subcritical crack-propagation conditions. Equant clasts with curviplanar margins are likely to have formed at low temperatures and low temperature differentials.
- Elongate, splinter- and wedge-shaped clasts are likely to have formed under high crack velocity in critical crack-growth regimes at high temperature differentials.
- Perlite cracking may be a product of thermal stressing and quenching under slow-cooling, subcritical conditions.
- Fine hyaloclastite breccia is the product of a fast cooling rate and high temperature differential, which is why hyaloclastite grainsize may vary from fine at the margins of a body to coarser in the interior and even grade into a coherent interior.
- Jig-saw fit textures are indicative of in situ, nonexplosive, cooling contraction quench fragmentation.
- Clast-rotated textures indicate postcrack formation movement as a result of continued lava or intrusion movement or downslope resedimentation.
- The grainsize of quench-fragmented crystalline glass hyaloclastite is likely to be coarser than for aphyric glass hyaloclastite.
- Pumice hyaloclastite should not be unusual in subaqueous settings and not all pumice is pyroclastic in origin.

In the following sections, we illustrate how some of the processes of subaqueous volcanism, in particular those regarding magma fragmentation and transport and deposition of volcanic debris, are recorded in the submarine volcanic rocks of Cabo de Gata.

3. Geological setting of Cabo de Gata

The Betic-Rif is a complex orogenic system whose geodynamic evolution has been widely debated (e.g., for recent reviews [18–20]). This complexity partly arises from the need to

http://dx.doi.org/10.5772/63579

reconcile the structures and kinematics of geodynamic processes operating at different scales and times in the narrow area of the western Mediterranean with the large-scale and long-standing geodynamic scenario of African and Eurasian plate convergence.

The Betic-Rif Orogen is an arcuate mountain belt with a northern branch formed by the Betic cordillera in the Iberian Peninsula and a southern branch formed by the Rif chain in northern Africa. The orogen displays a tight arc with a westward concavity in the Gibraltar strait (**Figure 1**). Igneous rocks of tholeitic, calc-alkaline, shoshonitic and ultrapotassic compositions show enrichment in K with time and are exposed in the internal areas of the belt [19, 21, 22]. Igneous rocks are subduction-related in a broad sense and are partly coeval with the extension tectonics developed in the internal areas of the Betic-Rif during Neogene. Calc-alkaline rocks in particular, display a clear arc-related geochemical signature and are synchronous with the opening of the back-arc Alborán basin (**Figure 1**). Arc curvature, arc magmatism and back-arc extension were formed during Miocene time by the westward rollback of a narrow eastward-subducting slab fragmented from the African plate [20, 22, 23]. Westward retreat of the subducted slab was accompanied by thinning of the continental crust, formation of oceanic crust and extension, leading to the formation of Neogene intramontane basins in the internal areas of the Betic-Rif [20, 22, 24]. Extension ceased in Late Miocene and deformation in the internal areas of the Betic-Rif was dominated by the kinematics of African and Eurasian plate convergence. NNW convergence of Africa with Iberia compressed the Alborán basin and reactivated suitably oriented faults in the intramontane basins. The internal areas of the Betic-Rif became a diffuse plate boundary between Africa and Eurasia dominated by wrench tectonics processes that are still active, as shown by recent seismicity of the Carboneras fault and other similar strike-slip faults [20, 22, 25].

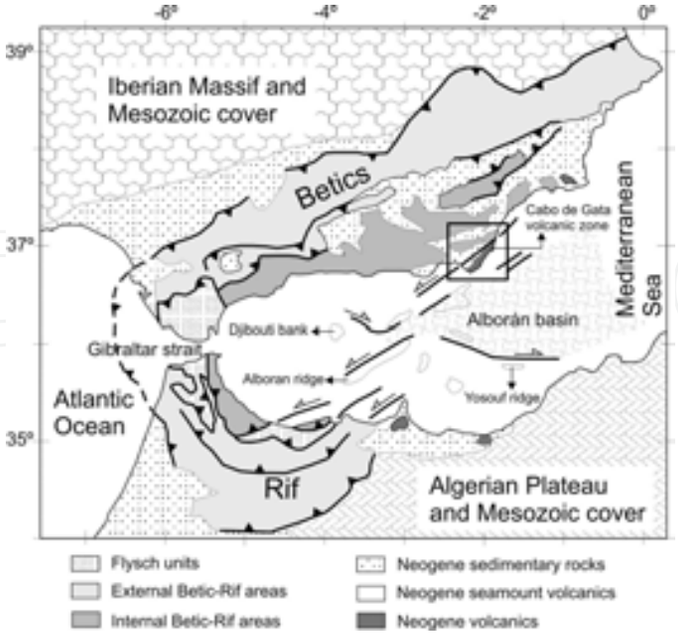

Figure 1. Geologic map of the Betic-Rif Orogen in the Western Mediterranean with location of the Cabo de Gata volcanic zone (modified from [24, 26]). Box shows location of **Figure 2**.

Due to the complex geodynamic evolution of the Betic-Rif Orogen and to the wrench tectonics established in the internal areas since Late Miocene time, the volcanic arc of the Betic-Rif appears distributed along fault-bounded seamounts in the Alborán Sea and onshore in volcano-sedimentary basins on both branches of the mountain belt (**Figure 1**). The Cabo de Gata volcanic zone corresponds to a portion of this volcanic arc exposed in the eastern part of the Almería-Níjar basin (**Figure 2**). This basin is structurally controlled by the Carboneras fault, which divides the basin into a western through dominated by Late Miocene to Pleistocene sedimentary rocks and an eastern through dominated by Miocene volcanic rocks (**Figure 2**). The Carboneras fault is an active structure with a complex kinematic history that includes contemporaneous strike-slip and dip-slip movements since Early Miocene time [27–29]. Basement to the Neogene succession of the Almería-Níjar basin are Paleozoic to Jurassic metamorphic rocks of the Maláguide, Alpujárride and Nevado-Filábride complexes that crop out in the mountain ranges bounding the basin (Sierra Cabrera, Sierra Alhamilla) and along the Carboneras fault strands (**Figure 2**). Gravimetric data and magnetic modeling suggest that volcanic rocks underlie Late Miocene to Pleistocene sedimentary rocks in the western part of the Almería-Níjar basin. The residual gravimetric anomaly together with well log data suggest that Neogene infill of the basin increases to the southwest (SW) and that the Neogene-basement boundary dips to the SW [30, 31]. The structure of the Almería-Níjar basin, of other intramontane basins of the Betic-Rif and of submarine promontories in the Alborán Sea consists of low-amplitude open folds with kilometer-scale wavelengths related to stepped normal faults, which are in turn associated with regional strike-slip faults [30, 32, 33].

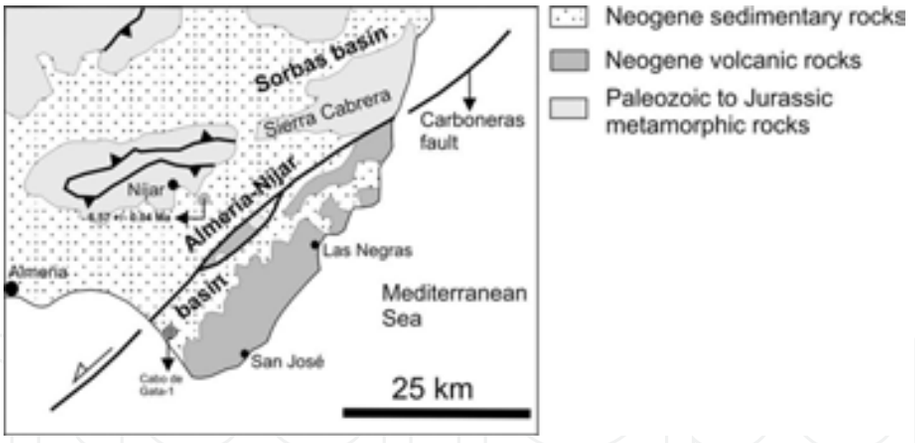

Figure 2. Simplified geologic map of the Almeria-Níjar basin and the Cabo de Gata volcanic zone (modified from [34]). Ar^{40}/Ar^{39} age corresponds to the Cerro del Hoyazo dacite [35].

4. Stratigraphy, geochronology, and structure of the Cabo de Gata volcanic zone

The Cabo de Gata volcanic zone is an area of semiarid climate in which rock exposure is virtually continuous both along the shoreline and the inland. Maximum elevation is nearly

http://dx.doi.org/10.5772/63579

500 m above sea level and the original morphologies of volcanic edifices are poorly preserved due to erosion. Nevertheless, excellent exposures of stratigraphic sections along marine cliffs and inland allow a precise reconstruction of the volcanic stratigraphy. Based on preserved exposures of deposits, Cabo de Gata can be understood as a volcanic field formed by dispersed small-scale lava domes and larger dome complexes and by larger volcanic seamounts. The stratigraphic succession of Cabo de Gata consists of volcanic rocks interbedded with sedimentary rocks, mainly carbonate and siliciclastic deposits. Bedding of volcanic and sedimentary rocks, dip of tabular lavas and overall disposition of volcanic bodies are subhorizontal or shallowly inclined to the northeast (NE), providing a general upward stratigraphic polarity toward the NE.

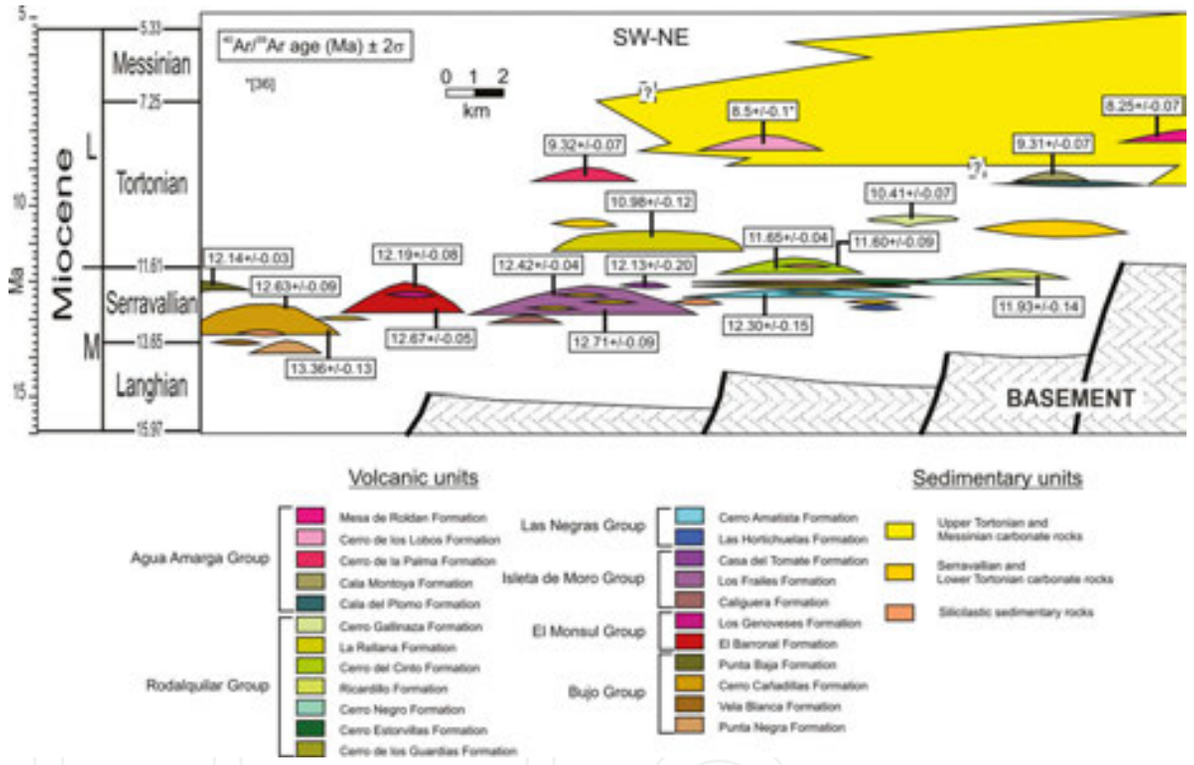

Figure 3. Chronostratigraphic scheme of the Cabo de Gata volcanic zone with distribution of the different lithostratigraphic units (modified from [10]). All Ar^{40}/Ar^{39} ages from [22] except [36].

The volcanic stratigraphy shown in **Figure 3** is a revision of that in [10] with some minor changes regarding the aggregation of formations into groups, in particular the Agua Amarga and Rodalquilar groups. Description, discussion and extended data on the Ar^{40}/Ar^{39} ages of formations are available in [22]. The lithostratigraphic units distinguished are formations formally defined that were subsequently divided into informal subunits when required [10]. The criteria used to divide the stratigraphic succession of Cabo de Gata into formations and to aggregate them into groups is based on lithology, stratigraphic position, age and geochemical affinity. Formations, groups and the informal units within formations are bounded by unconformities of different hierarchy. Volcanic units are interbedded with sedimentary units throughout the Cabo de Gata region with an overall trend of thicker and older volcanic units

toward the SW and thicker and younger sedimentary units toward the NE (**Figure 3**). Upper Tortonian to Messinian sedimentary rocks cap the volcano-sedimentary succession toward the NE. Sedimentary units are laterally discontinuous, in particular toward the SW of Cabo de Gata, which may result in the local amalgamation of thick piles of volcanic rocks separated by unconformities.

The main structural features in Cabo de Gata are subvertical normal faults that affect volcanic and sedimentary units and can be grouped into three sets based on their orientation: dominant NW-SE- to N-S-trending faults and subordinate NE-SW-trending faults (**Figure 4**). Fanning stratal dips and differences in bed thickness across fault blocks are thought to indicate that displacement along some faults is syndepositional to the emplacement of volcanic and sedimentary rocks [32]. Epithermal ore deposits of the Rodalquilar mine area result from hydrothermal fluids precipitated at high temperatures along N-S-trending faults [6]. Structures in Cabo de Gata are similar to those of other Neogene intramontane basins of the Betic Rif Orogen and of volcanic seamounts of the Alborán Sea. These structures are associated with the still active wrench tectonics established in the area since Late Miocene. This tectonic regime is ultimately responsible for the observed uplift-downlift displacements along some faults and for the present-day exposure above sea level of the submarine volcano-sedimentary successions of Cabo de Gata.

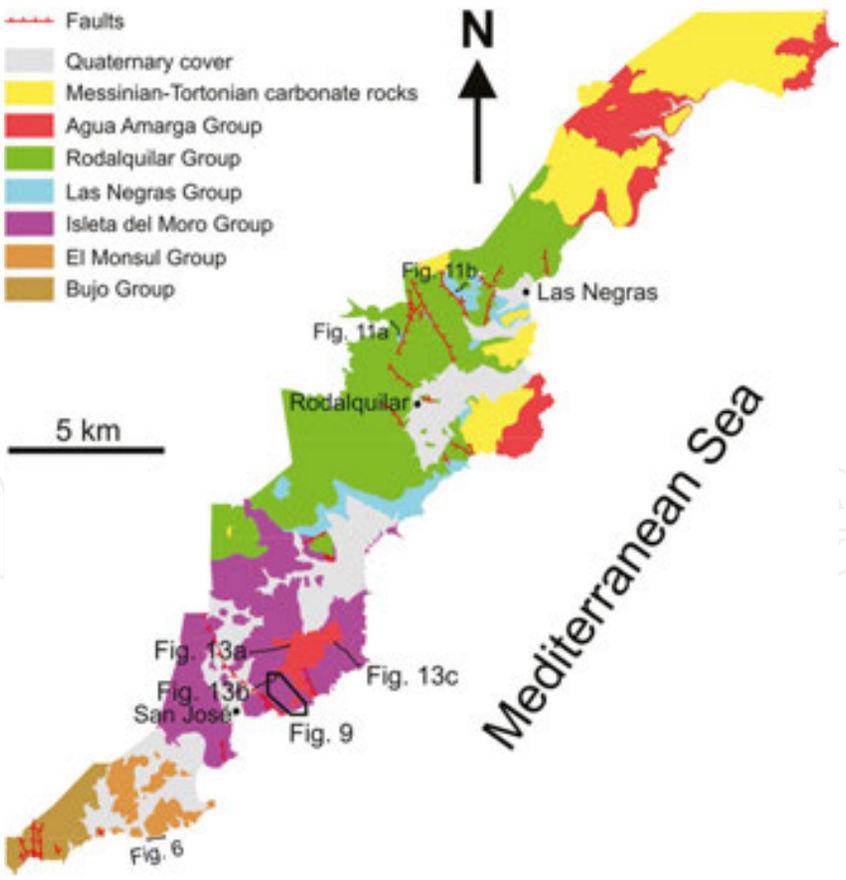

Figure 4. Simplified geologic map of the Cabo de Gata volcanic zone with the distribution of groups and location of figures (modified from [22]).

http://dx.doi.org/10.5772/63579

The chronostratigraphic position of volcanic units based on radio-isotopic ages indicates that volcanism in Cabo de Gata started in Serravalian and ended in Tortonian times (**Figure 3**). During this time, volcanism migrated toward the NE while hiatuses in the volcanic activity became increasingly significant (**Figure 5**). Geophysical and well-log data reveal the occurrence of volcanic rocks beneath the oldest dated unit of Cabo de Gata [30, 31]. Hence, given the Messinian age of the Cerro del Hoyazo dacite [35], the volcanic activity in the whole Almeria-Níjar basin may have encompassed Middle to Late Miocene time (**Figure 5**). Volcanic formations and informal subunits within them correspond to volcanic cycles in a wide sense, meaning that they include all the deposits associated with the volcanic activity during an eruptive period. The volcanic units are separated from each other either by distinct unconformities or by sedimentary rocks, indicating hiatuses in the volcanic activity and erosion of volcanic edifices and deposits. In the following sections, the relevant features of Cabo de Gata volcanism are illustrated with selected examples of deposits and stratigraphic successions.

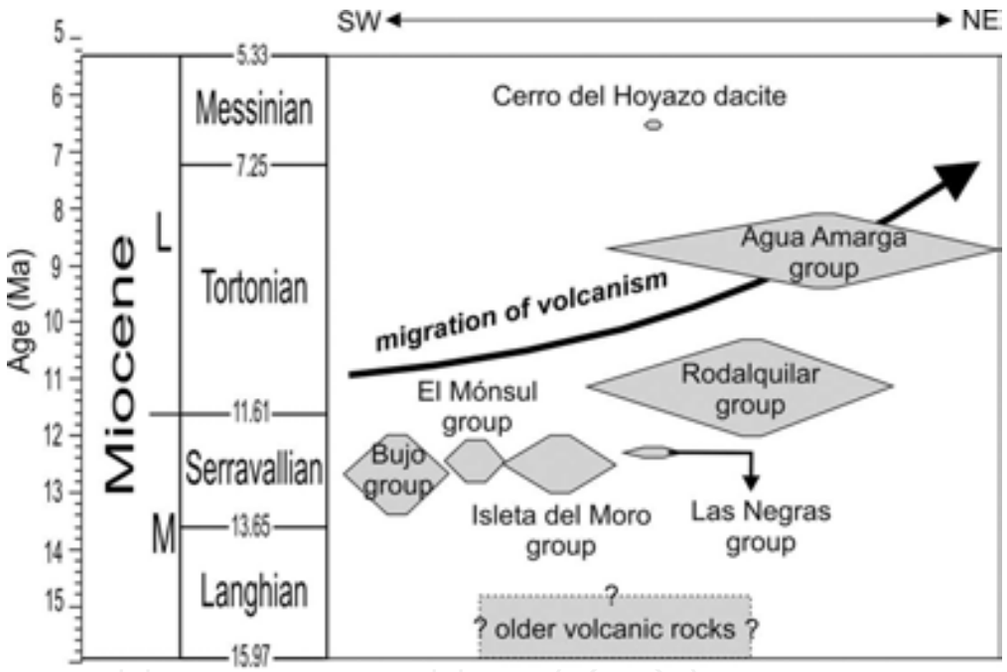

Figure 5. Chronologic timetable of the volcanic activity in the Almería-Níjar basin based on Ar^{40}/Ar^{39} ages of dated rocks approximately distributed from SW-NE (modified from [22]).

5. Transitions between explosive and effusive conditions during submarine eruptions

Transitions from explosive to effusive activity or vice versa are common during individual eruptions in most subaerial volcanoes (Teide, Soufrière Hills, Mount St. Helens, Monte Pilato, etc.). Transient conditions during eruptions have been either witnessed in active volcanoes or are well documented through the study of volcanic deposits. In subaqueous settings, however,

their study is certainly more problematic and the usually incomplete and fragmental nature of many submarine successions hampers a proper understanding of how these transitions are recorded. Here, transitions from explosive to effusive eruptive style during individual eruptions are illustrated with examples from the volcanic succession of the El Barronal Formation in southwestern Cabo de Gata (**Figure 4**). An extended description of the lihofacies succession of this unit is available in [9].

The El Barronal Formation consists of a succession of lavas interbedded with volcaniclastic rocks that is intruded by subvertical dikes (**Figure 6**). The lower boundary of this unit is an unconformity with the Cerro Cañadillas Formation while the upper limit is not exposed. The whole El Barronal Formation is composed of up to five lava units. The El Barronal Formation has been Ar^{40}/Ar^{39}-dated at 12.19 Ma for lava unit 4 and 12.67 Ma for lava unit 3 [9]. Interbedded between these two lava units is the rhyolitic dome of the Los Genoveses Formation and also carbonate rocks with shell fragments and polymictic siliciclastic rocks with rounded pebbles from the metamorphic basement of the Neogene succession of Cabo de Gata (**Figure 3**).

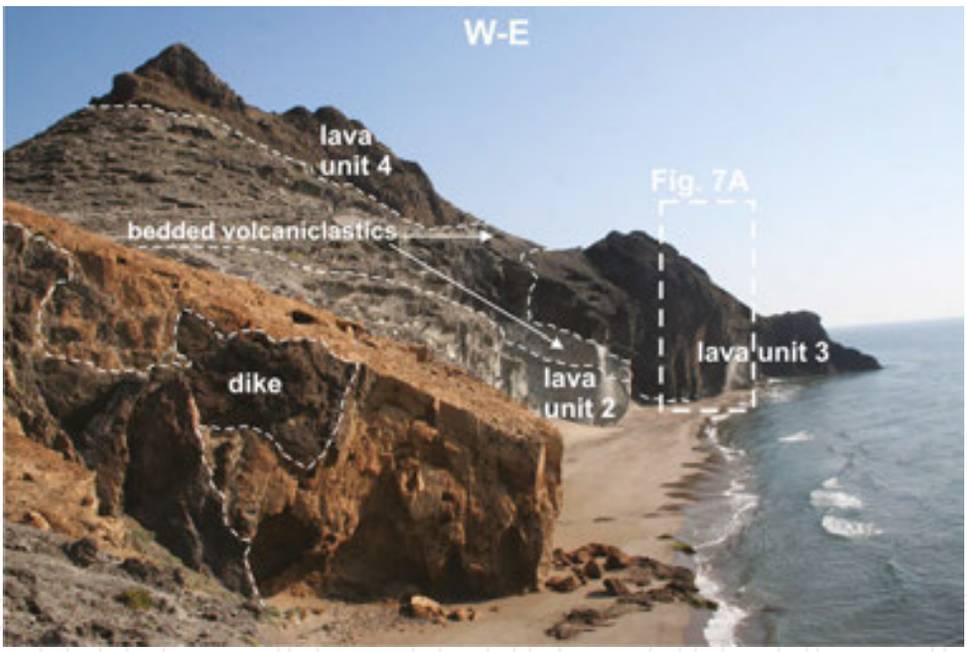

Figure 6. Panoramic view of the stratigraphic succession of the El Barronal Formation at Playa del Barronal. Note lava unit 3 pinching out into bedded volcaniclastic succession to the west (see **Figure 4** for location).

Lavas, volcaniclastic rocks and dikes of the El Barronal Formation have identical andesitic composition and mineralogy. Lavas are formed by a coherent core grading into an outer carapace of in situ to clast-rotated hyaloclastite breccia. The coherent core of lavas has colonnade columnar joints and entablature columnar joints usually forming rosette structures (**Figure 7A**). The outer carapace consists of massive hyaloclastite with dense clasts grading outward into massive and flow-banded hyaloclastite with vesicular clasts (~40% vesicles). Volcaniclastic rocks are bedded and consist of massive breccia with dense and vesicular clasts, diffusely bedded pumice-rich breccia, cross-bedded crystal-rich sandstone and thinly bedded

http://dx.doi.org/10.5772/63579

fine tuffaceous sandstone. These facies types contain outsized clasts and have rapid vertical and lateral transitions between them (**Figure 8**).

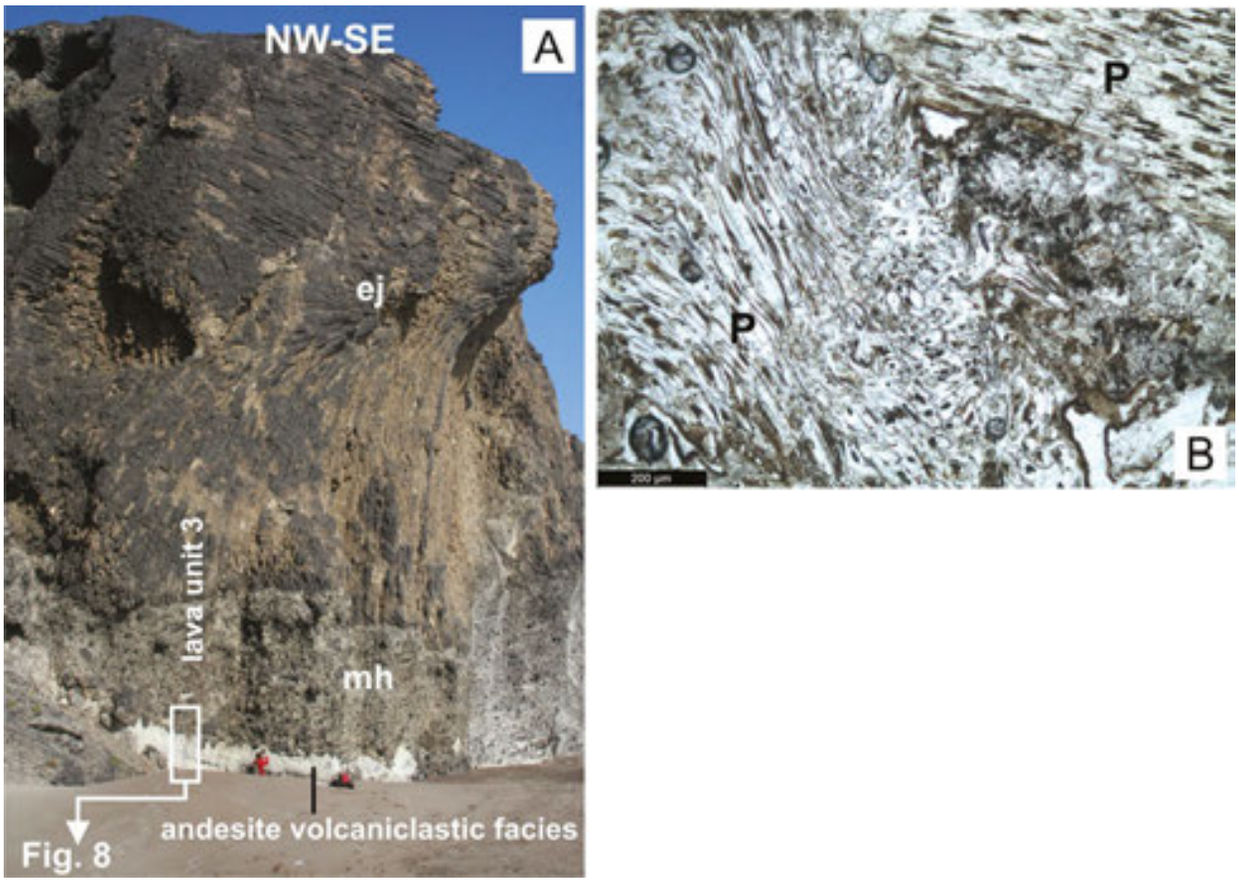

Figure 7. A: lava unit 3 of the El Barronal Formation with entablature jointed facies (ej) showing fan-like joints and grading downward into massive hyaloclastite with dense clasts (mh) and **B**: photomicrograph of finely bedded tuffaceous sandstone with tube-pumice clasts (P).

Volcaniclastic facies contain a variety of clasts indicating provenance from different sources: juvenile components (pumice clasts, glass shards and crystals), clasts derived from underlying lavas (dense rock clasts and vesicular clasts) and exotic well-rounded andesite cobbles likely derived from sources above wave base. Juvenile components are rare in massive breccia, whereas they are present in different amounts in the rest of volcaniclastic facies. Textural evidence of juvenile clasts (i.e., vesicularity >60%, tube-pumice clasts and bubble-wall shards) suggests fragmentation of magma in the conduit by magmatic explosions, whereas the blocky shape of crystals and lithics can be attributed to some degree of magma-water interaction in the fragmentation processes (**Figure 7B**). Finer-grained volcaniclastic facies show distorted bedding, small-scale faults, folds and dish structures, suggesting that they were water-saturated at emplacement. Soft-sediment deformation structures are invariably located at the contact between volcaniclastic facies and upper lavas indicating that volcaniclastic facies were wet and poorly consolidated at the emplacement of upper lavas (**Figure 8**). These contact relations suggest that the time encompassed between the deposition of volcaniclastic facies

and the emplacement of upper lavas was short and that lavas and volcaniclastic rocks were likely syn-eruptive.

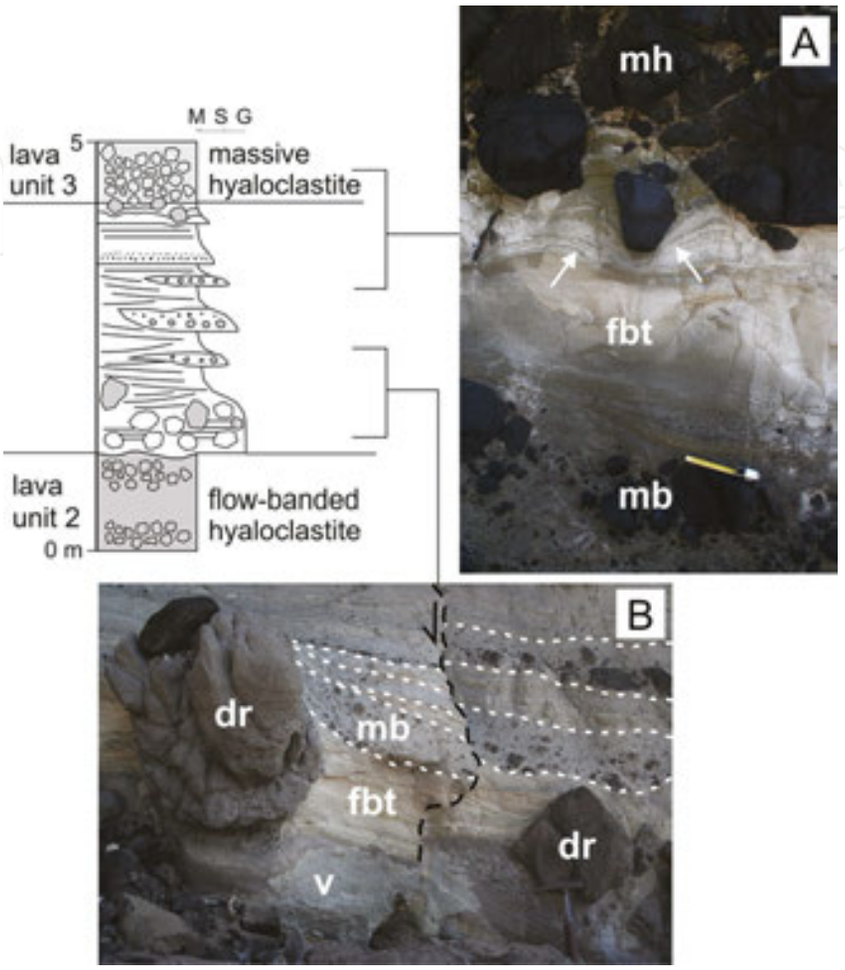

Figure 8. Stratigraphic log and contact relations of the volcaniclastic deposits located between lava unit 2 and 3 of the El Barronal Formation. mh, massive hyaloclastite; mb, massive breccia; tbt, thinly bedded fine tuffaceous sandstone; dr, dense rock clast; v, vesicular clast (see **Figure 7A** for log location).

The El Barronal Formation can be characterized as a succession of eruptive cycles, each of which started with explosive eruptions that yielded deposition of volcaniclastic facies and ended with the effusive emplacement of lavas. A hiatus in the andesite volcanic activity of El Barronal, with eventual deposition of carbonate sediments and emplacement of rhyolitic magma, separates each volcanic cycle. Explosive activity was complex as suggested by the rapid lateral and vertical transitions among volcaniclastic facies and by coexistence of textural evidences indicating fragmentation of magma by magmatic explosions and by magma-water interaction processes. The latter would have enhanced fragmentation efficiency yielding the grain size of finer volcaniclastic facies. Explosive eruptions may have mixed together the different types of juveniles, lithics and clasts from above-wave-base settings too. Steam-driven explosions would have been responsible for the fragmentation of blocks and smaller clasts and the deposition of massive breccia.

http://dx.doi.org/10.5772/63579

6. Submarine volcanic debris-avalanche deposits

Collapse of volcanic edifices and deposition of debris-avalanche deposits in submarine settings are common processes. They often partially affect ocean-island volcanoes such as Hawaii, Tenerife, Reunion and Augustine and also submarine volcanic edifices such as lava domes and stratovolcanoes. Most of the debris avalanches under the sea are inaccessible for obvious reasons and their study has to be undertaken indirectly by means of different geophysical techniques. To our knowledge, there is only one volcanic submarine debris avalanche deposit described in the literature that has been studied in detail by direct access to onshore exposures [37].

The volcanic debris avalanche deposits of Cabo de Gata are well exposed and fairly well constrained in terms of their submarine depositional setting. Therefore, they constitute a unique opportunity for a direct study of this kind of deposits. Here we summarize the main characteristics of two debris avalanche deposits in Cabo de Gata, one of which has been already described in a former work [8] and is the subject of ongoing research.

6.1. The debris avalanche deposits of the Los Frailes Formation

Submarine volcanic debris avalanche deposits crop out to the northeast of San José village in southern Cabo de Gata (**Figure 4**). These deposits are stratigraphically located in informal subunits 2 and 4 of the Los Frailes Formation. Ar^{40}/Ar^{39} ages of sampled blocks from the debris avalanche deposits in subunits 2 and 4 are 12.71 Ma and 12.42 Ma, respectively.

The debris avalanche deposit of subunit 2 is particularly well exposed and is bounded by upper and lower carbonate sedimentary rocks that are laterally discontinuous and contain oysters, corals, echinoderms, algae, and undifferentiated shell fragments (**Figure 9**). This debris avalanche deposit is laterally associated to the northwest with dacite lavas showing a flow-banded and columnar-jointed coherent core that grades outward into in situ to clast-rotated hyaloclastite breccia (**Figure 9**). Lavas and debris-avalanche deposit have identical dacite composition and mineralogy. The debris-avalanche deposit of subunit 2 is massive and monomictic and has an internal organization consisting of block facies "floating" in matrix facies or mixed facies (**Figure 10A**), which is consistent with the classical descriptions of debris avalanche deposits in the literature [38–40]. Some blocks are up to 10^4 cubic meters, although most of them are usually about an order of magnitude smaller and most blocks have a flow-banded and polyhedral-jointed interior (**Figure 10B**). The basal contact of megablocks is sharp, planar, and often fractured with dislocations showing stepped geometry. Shear planes with sigmoid shape form anastomosed lenses and are common at the base of megablocks (**Figure 10C**). Matrix consists of a clast-supported framework of centimeter- to decimeter-size angular clasts with randomly oriented internal flow banding (**Figure 10B**). The upper surface of the debris avalanche deposit in subunit 2 is flat, whereas the lower surface is more irregular, gently dipping to the SE in the northwestern part (**Figure 9**). The maximum thickness of this deposit is nearly 100 m. If a map view of the upper surface of the deposit was exposed rather than an oblique cross-section of the whole deposit, the positive

topography built up by megablocks would have likely resulted in the classical hummocky morphology of most debris avalanche deposits [38, 41, 42].

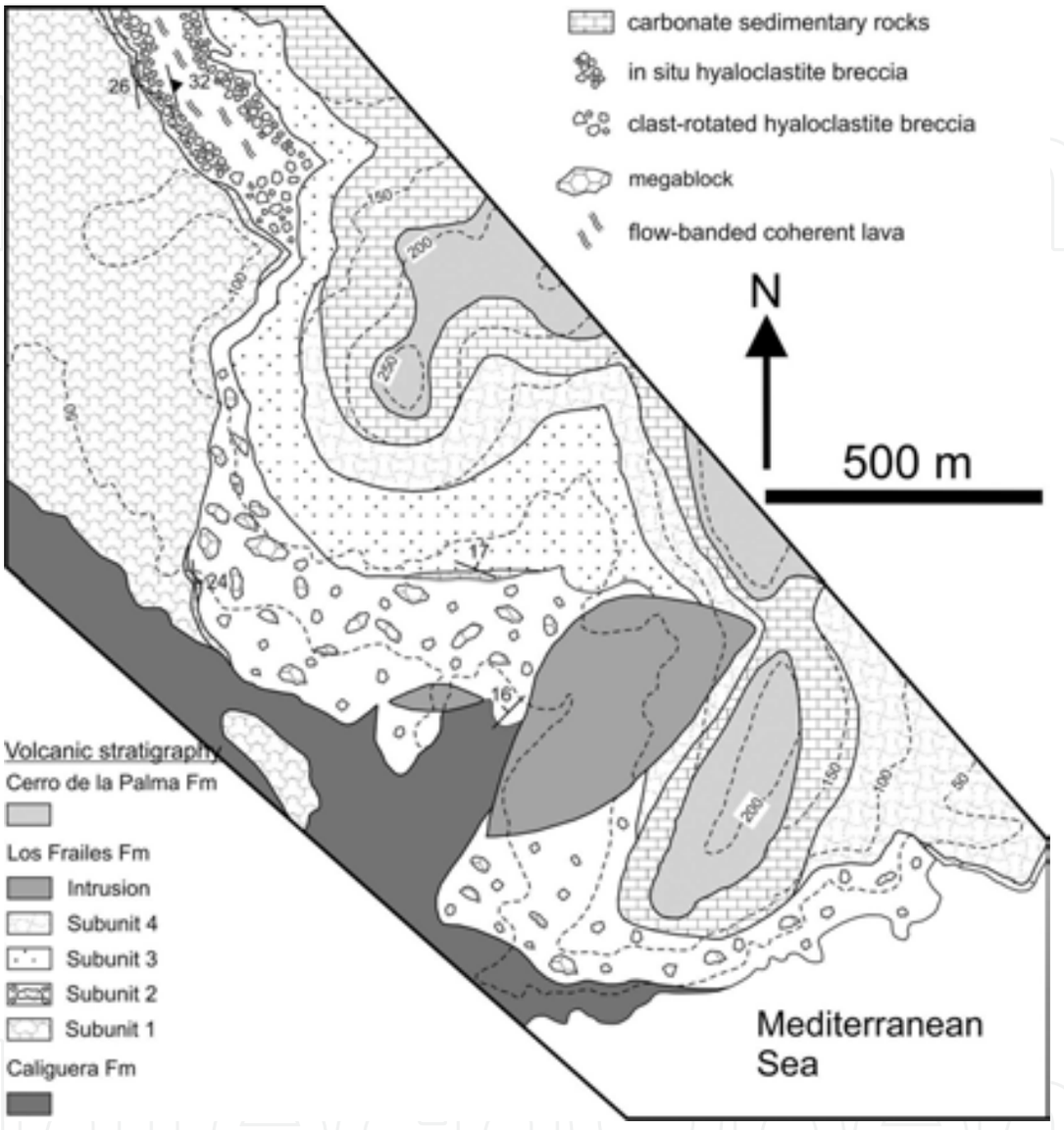

Figure 9. Geologic map of the Los Frailes Formation (see **Figure 4** for location).

The lateral association of the debris-avalanche deposit and lavas within subunit 2, together with their identical composition and mineralogy, indicates that dacite lavas are probably the source area for the volcanic debris of the avalanche deposit. Thickness and areal distribution of the debris-avalanche deposit in **Figure 6** and nearby areas suggests a volume <0.5 km^3 and run-out distance <5 km [8]. These factors together suggest that the debris avalanche is derived from the sector collapse of a submarine lava dome or a dome complex. In this view, megablocks correspond to the coherent core of the lava dome, whereas matrix facies corresponds to the hyaloclastite carapace surrounding the core. In spite of this general provenance for block and matrix facies, block disintegration and clast-to-clast friction during transport are not to be

http://dx.doi.org/10.5772/63579

excluded as mechanisms producing block and clast fragmentation [42, 43]. This is particularly evident by the shear deformation and stepped geometry at the base of megablocks.

The debris-avalanche deposit of subunit 4 is thinner and less extended laterally than that of subunit 2. It is massive, monomictic and dacitic in composition and is stratigraphically limited by lower and upper carbonate sedimentary rocks that contain marine fossils. The internal organization of the debris avalanche deposit of subunit 4 is similar to that of subunit 2, consisting of block and mixed facies.

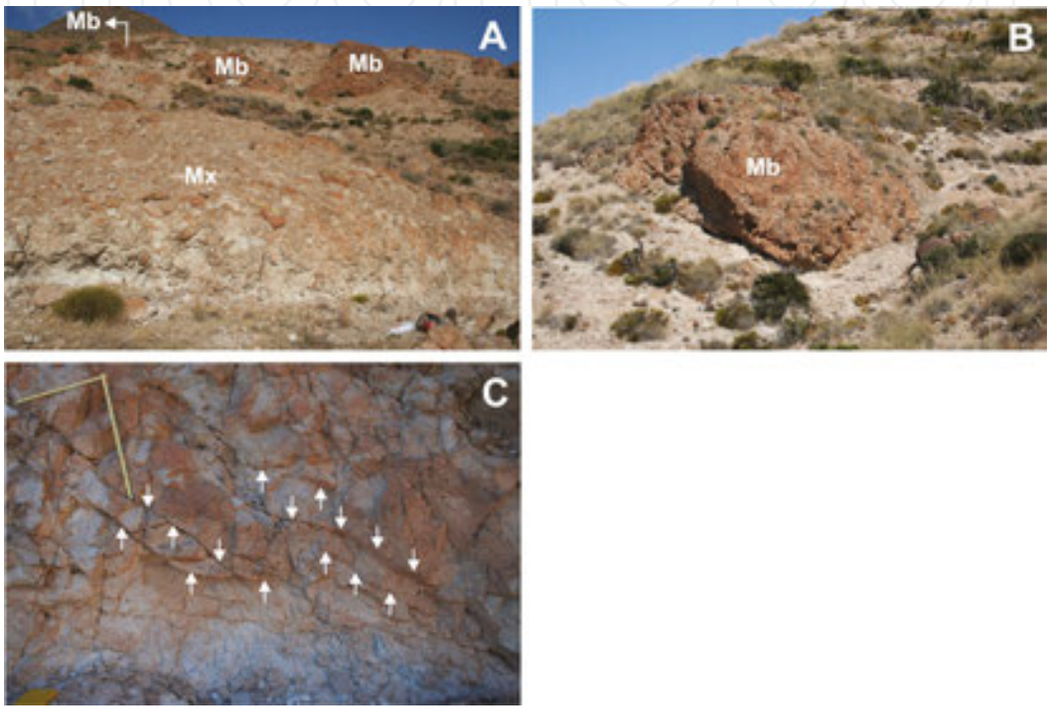

Figure 10. A: panoramic view of the debris-avalanche deposit of subunit 2 of the Los Frailes Formation with megablocks (Mb) and matrix (Mx). **B**: megablock with polyhedral-jointed interior and sharp basal contact. **C**: base of a megablock with anastomosed sigmoid shear planes (arrows).

6.2. The debris avalanche deposit of the Cerro Estorvillas Formation

Inland exposures to the west of Las Negras and to the north of Rodalquilar in the central Cabo de Gata area provide well-preserved profiles of the debris avalanche deposit of the Cerro Estorvillas Formation (**Figure 4**). This unit uncomformably overlies rhyolite bedded pumice breccia of the Cerro de los Guardias Formation and is unconformably overlain by flow banded dacite lavas of the Monte Cinto Formation and by andesite lavas and breccias of the Cerro Negro Formation. The age of the Cerro Estorvillas Formation is stratigraphically constrained between 12.30 Ma and 11.93 Ma (**Figure 3**). The Cerro Estorvillas Formation is dacitic in composition and monomictic and consists of a volcanic succession with a debris avalanche deposit at the base grading upward into bedded pumice breccia that in turn grades upward into bedded and massive breccia (**Figure 11**). To the west of Las Negras, the Cerro Estorvillas Formation also includes dacite lavas.

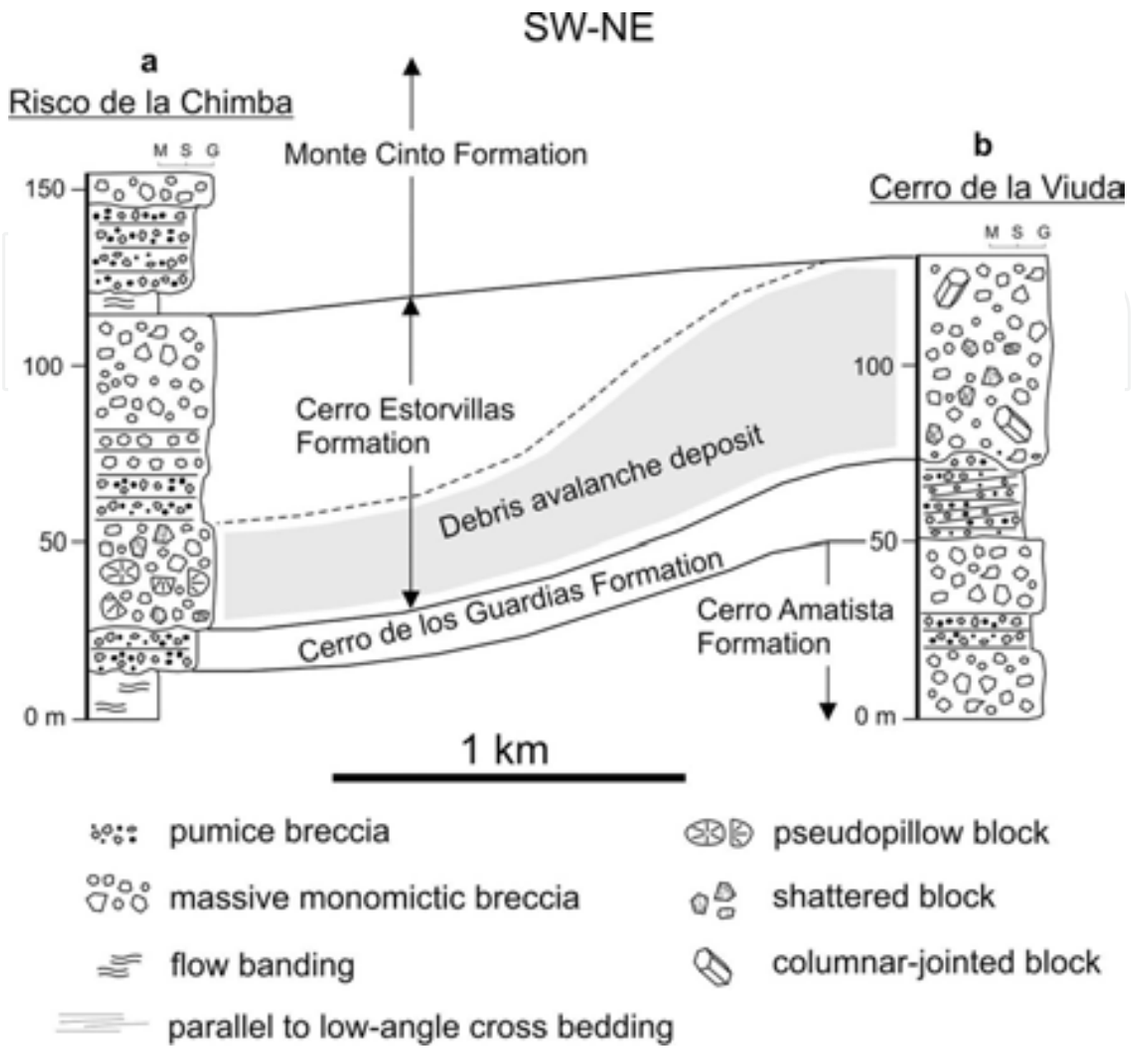

Figure 11. Stratigraphic logs of the Cerro Estorvillas Formation (see **Figure 4** for log location).

The debris avalanche deposit of the Cerro Estorvillas Formation is almost 100 m thick near Las Negras, whereas it is less than 50 m thick farther to the west. This deposit is massive and internally organized in block and mixed facies. Block facies consists of angular clasts up to 6 m across, including meter-size pseudopillow blocks that exhibit radial jointing and meter-size blocks with columnar jointing (**Figure 12A** and **B**). Mixed facies comprises a clast-supported framework of centimeter- to decimeter-size angular clasts of the same composition and mineralogy as the blocks. Blocks are usually shattered with a jigsaw-fit fracture framework. In the lower part of the debris-avalanche deposit, irregular domains with diffuse margins extend laterally for more than 10 m and are less than 5 m thick. These domains consist of well-rounded cobbles of dacite occasionally supported in a matrix of coarse sand that consists of dense rock fragments of dacite and crystals (**Figure 12C**). The contact of the debris avalanche deposit with the underlying Cerro de los Guardias Formation consists of an irregular zone in which clasts and small, usually vein-like, portions of the debris avalanche deposit are mixed with clasts and portions of the underlying pumice breccia deposit (**Figure 12D**). This mixing zone extends up to 2 m upward from the basal contact of the debris-avalanche deposit.

http://dx.doi.org/10.5772/63579

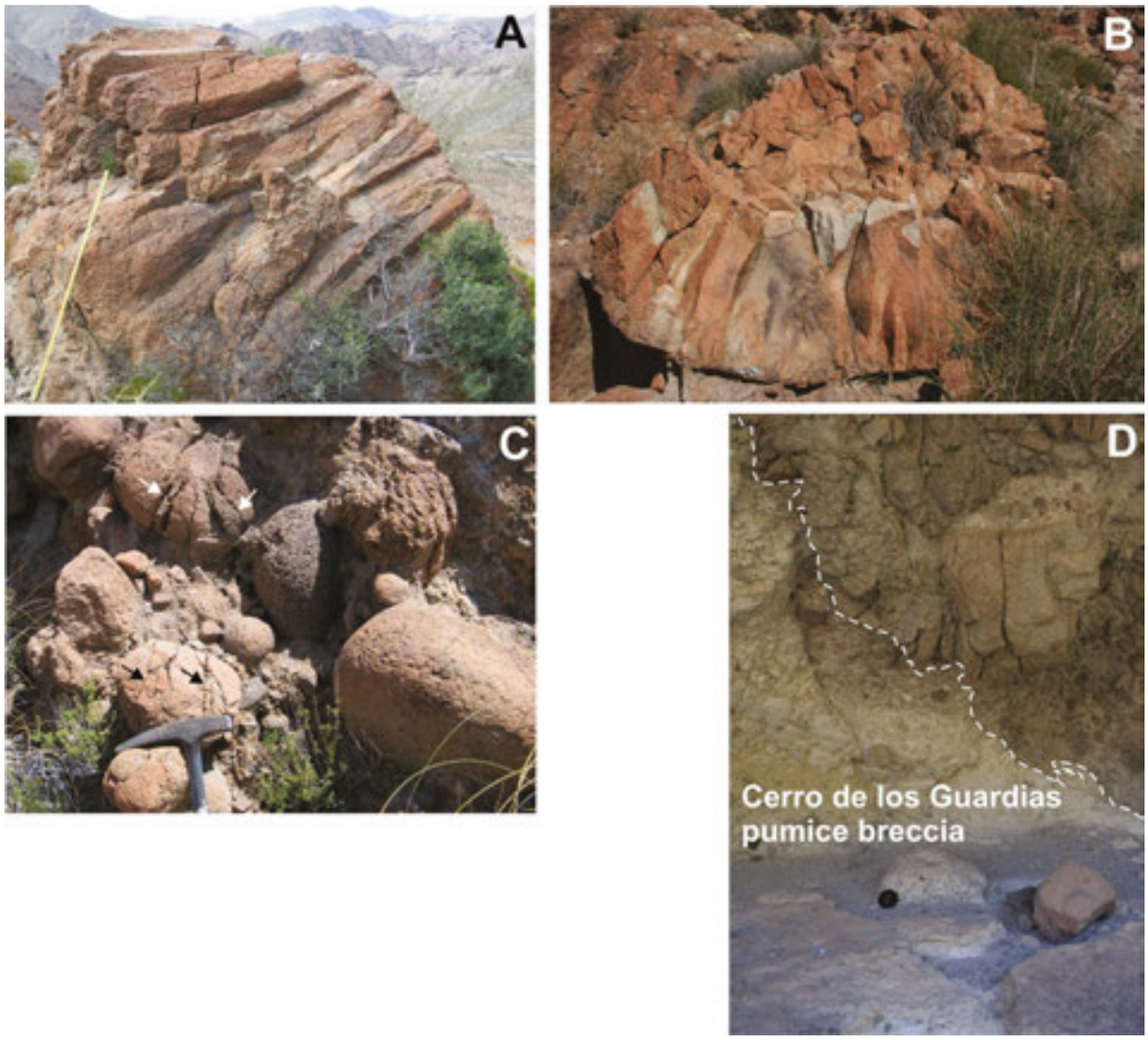

Figure 12. **A**: columnar-jointed block in the debris-avalanche deposit of the Cerro Estorvillas Formation; **B**: pseudopillow block with radial jointing; **C**: detailed of the cobble domain in the lower part of the debris-avalanche deposit. Note fracture pattern in shattered cobble clasts (arrows); **D**: basal mixed contact of the debris-avalanche deposit of the Cerro Estorvillas Formation to the pumice breccia of the Cerro de los Guardias Formation. Note shattered clasts in the debris-avalanche deposit.

Lack of sorting, massive character, internal organization in block and mixed facies and shattered blocks with jigsaw-fit fractures are usual features of debris avalanche deposits [38, 40, 44, 45]. Pseudopillow radial-jointed blocks may derive from pillows and lava lobes surrounded by hyaloclastite breccia originally deposited in subaqueous settings while the monomictic character indicates a homogenous source for the volcanic debris. Rounded cobbles must have been formed by long-term reworking in highly energetic settings rather than in a nearly instantaneous event like a debris-avalanche. Although marine fossils have not been observed in the cobble domains, rounding of the clasts and the coarse sand matrix fits well with original deposition in a beach environment and subsequent transport within the debris

avalanche. Transport and deposition of nearly intact parts of the volcano stratigraphy is a common feature observed in many debris avalanche deposits [39, 41]. Hence, the debris avalanche of the Cerro Estorvillas Formation may have involved the partial collapse of an emerged dacite lava dome likely located to the west of Las Negras, where dacite lavas of the same composition and mineralogy occur. Rhyolite pumice and andesite clasts and irregular portions of pumice breccia from the underlying Cerro de los Guardias Formation at the basal contact of the debris avalanche are interpreted to have been ripped up from the substrate during transport.

7. Tectonic controls on cyclic volcanism

The nearly continuous sedimentation in passive-margins and other types of sedimentary basins allows characterization of basin dynamics by use of the principles of sequence stratigraphy and techniques such as backstripping and decompaction on sedimentary successions. In contrast, the record of volcanism is discontinuous in the geologic history due to its episodic character, whereas volcanic rocks allow a reasonably good determination of absolute ages via radio-isotopic dating. Additionally, in the coherent lithofacies of volcanic successions, compaction effects on accumulated thicknesses are minor and can be likely disregarded.

In Cabo de Gata, volcanic units were emplaced in submarine settings at unknown depth and are interbedded with sedimentary units in which paleobathymetry can be better constrained by analyzing the lithofacies of sedimentary successions. Using the known thickness and ages of volcanic rocks and the better-constrained paleodepth deposition of sedimentary rocks, the paleobathymetric setting of volcanism can be indirectly constrained and the uplift-downdrop history of volcano-sedimentary successions in Cabo de Gata can be roughly assessed. In addition, lateral correlation of the different lithofacies forming subunits of the Los Frailes Formation allows characterization of the eruptive styles and interpretation of the constructive and destructive processes of volcanic edifices during the eruptive periods. This may serve to illustrate the tectonic controls on cyclic volcanism not only of the Los Frailes Formation but also of other units in Cabo de Gata.

Debris-avalanche deposits of subunits 2 and 4 are laterally associated toward the north with coherent lava that grade into hyaloclastite breccias (**Figure 13**). Subunit 1 is also made up of debris-avalanche deposits and coherent lava that grade into hyaloclastite breccia and have a similar dacitic composition and mineralogy to dacite of subunits 2 and 4. Subunit 3 is made up of pumice-rich and glass-shard-rich lithofacies (i.e., massive and bedded pumice breccia, massive pumice tuff and thinly bedded fine tuff). Lithofacies of subunit 3 are fines depleted, have low-angle cross bedding and soft-sediment-deformation structures and show similar dacitic composition and mineralogy to subunits 2 and 4. Although subunit 3 is laterally discontinuous, it constitutes a distinctive stratigraphic marker in the Los Frailes area that allows lateral correlation of subunits within the Los Frailes Formation (**Figure 13**).

http://dx.doi.org/10.5772/63579

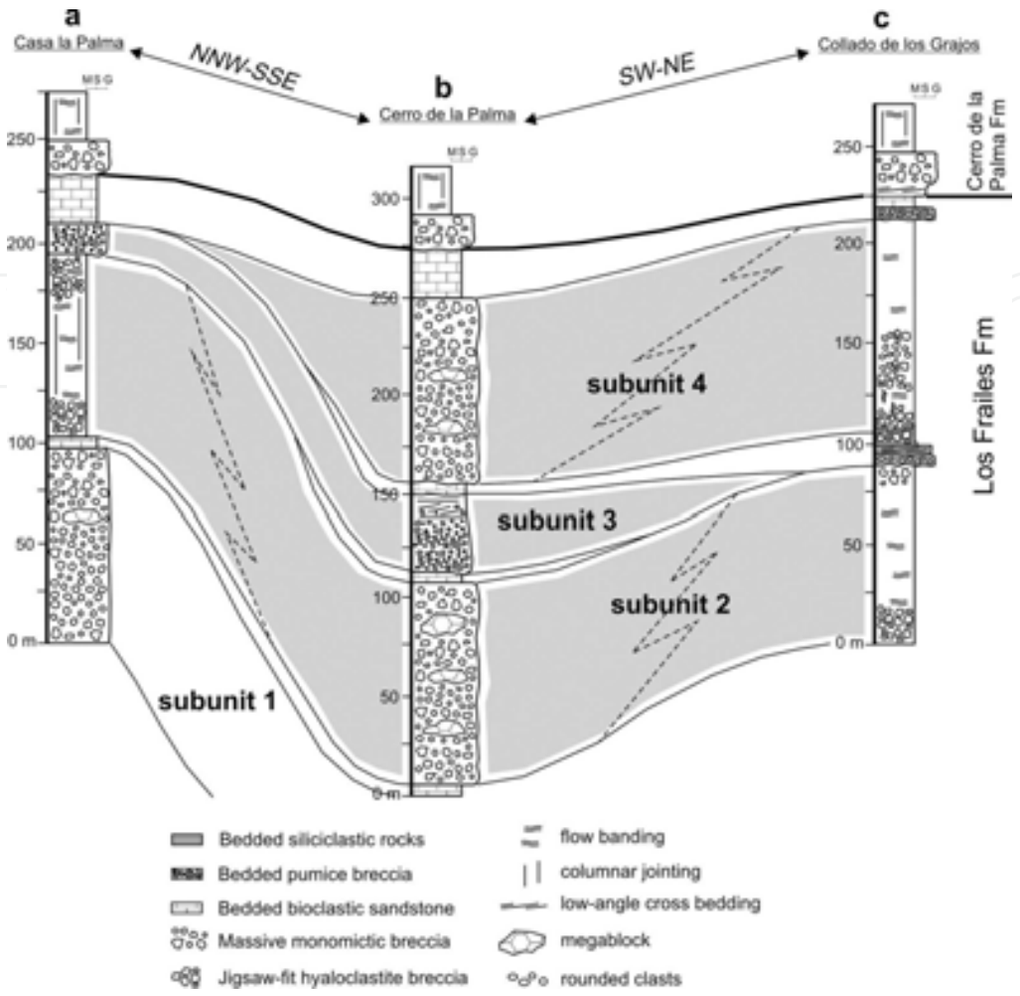

Figure 13. Correlation of volcanic subunits and sedimentary units of the Los Frailes Formation in the Los Frailes area (see **Figure 4** for log location).

At Collado de los Grajos, lava of subunit 2 is overlain by a fining-upward siliciclastic succession that, from base to top, consists of massive conglomerate with well-rounded pebbles of phyllite from the metamorphic basement to the Neogene succession of Cabo de Gata, low-angle cross-bedded coarse sandstone and cross-laminated fine sandstone to siltstone. The siliciclastic succession is overlain by lava of subunit 4, which consists of hyaloclastite breccia grading upward into coherent lava. Fine sandstone and siltstone of the upper siliciclastic succession fluidized and filled the space between clasts of in situ to clast-rotated hyaloclastite breccia of subunit 4. Coherent lava of subunit 4 is capped by a fining- and thinning-upward succession that, from base to top, includes a conglomerate bed, rhodolith-rich facies and cross-bedded sandstone (**Figure 14A**). The conglomerate bed is horizontal, up to 1 m thick and grades upward into a carbonate bed of up to 50 cm thick. The base of the conglomerate bed is irregular on the coherent dacite lava of subunit 4. Conglomerate is composed of well-rounded dacite cobbles with the free space among cobbles filled up with carbonate material infiltrated from the overlying carbonate bed (**Figure 14B**). Dacite cobbles and the underlying coherent lava are remarkably reddish. The upper carbonate bed is massive to crudely bedded and grades

upward into low-angle, cross-bedded bioclastic sandstone up to 25 cm thick. The carbonate bed is a rhodolith-rich rudstone that contains angular volcanic clasts, serpulids, bryozoan, bivalve fragments and other bioclasts (**Figure 14C**). Rhodoliths have a concentric algal framework around bioclastic nuclei and occasionally around volcanic clasts. The carbonate succession is overlain by cross-bedded monomict sandstone, massive monomict breccia and coherent lavas of the Cerro de la Palma Formation (**Figure 13**).

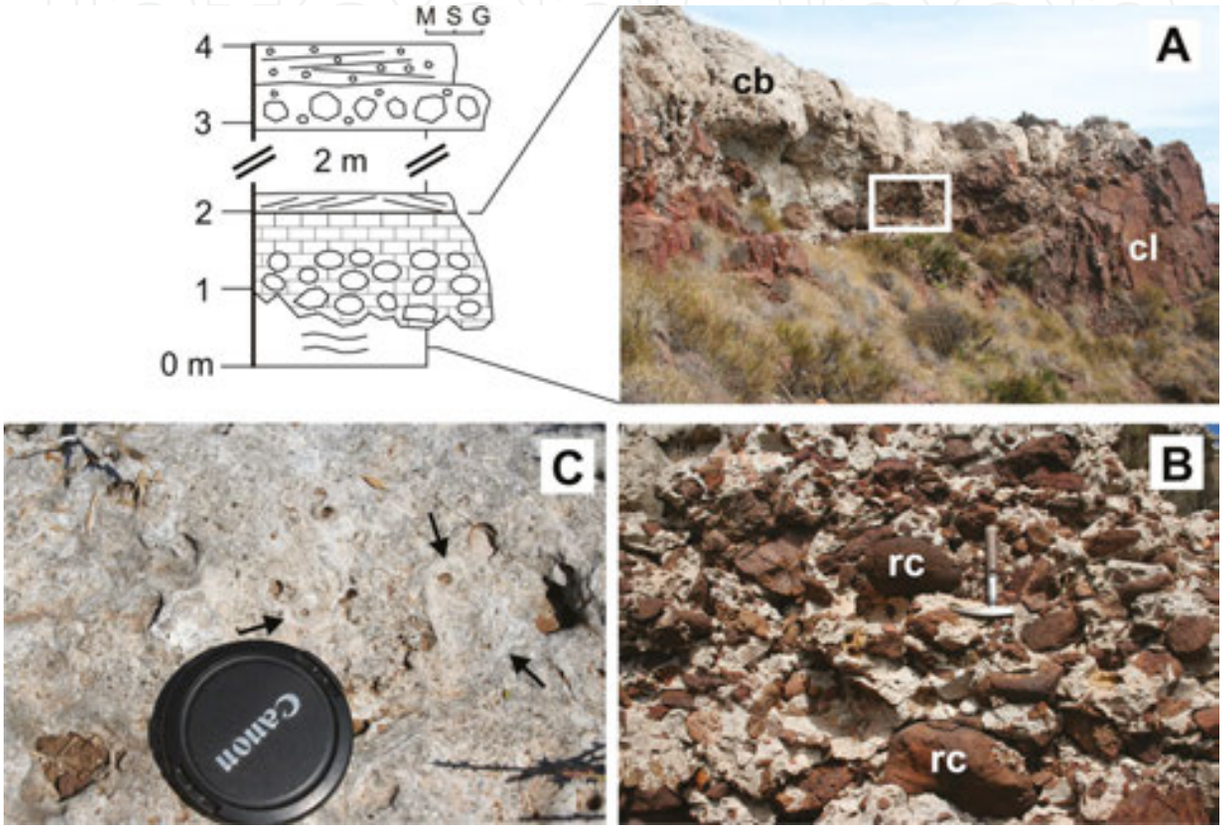

Figure 14. Detailed stratigraphic log of with the sedimentary sequence overlying coherent lava of subunit 4 in the Collado de Los Grajos log (see **Figure 13** for location). **A**: contact of subhorizontal conglomerate bed and carbonate bed (cb) on reddish coherent lava (cl). **B**: conglomerate bed with well-rounded cobbles (rc) and carbonate matrix infilling the the space among cobbles. **C**: top view of the carbonate bed with crustose rhodoliths forming concentric algae framework (arrows).

Fluidized sandstone and siltstone at the base of lava of subunit 4 indicates that the sediment was wet and nonconsolidated at the time of lava emplacement. The reddish color of the uppermost part of coherent lava of subunit 4 and of dacite cobbles of the upper conglomerate bed can be attributed to oxidizing conditions either at lava emplacement or after emplacement. Rhodoliths are encrusting coralline algae usually associated with above wave base environments, although they have been also described in deeper water settings [46, 47]. In terms of modern sequence stratigraphy, rhodolith-rich facies deposited on unconformities have been interpreted as condensed beds, indicating the onset of marine transgression ([48] and references therein). This interpretation fits well with the conglomerate bed on coherent lava of subunit 4 as deposited in a beach environment after lava emplacement and with rhodolith-

http://dx.doi.org/10.5772/63579

rich bed and cross-bedded sandstone as a deeper facies in an ongoing marine transgression. Hence, the fining and thinning-upward sedimentary sequence with the conglomerate bed at the base and the cross-bedded sandstone at the top is interpreted to have been deposited above wave base and to reflect deepening water conditions from the shoreface down to infralittoral settings. The depositional model of a Late Holocene clastic prograding wedge in the western Mediterranean has been studied in detail and shows that the mean storm wave base is 20 m below sea level [49]. The present-day configuration of the western Mediterranean was somewhat similar to the paleogeographic configuration in early Tortonian times, in which the Mediterranean Sea was connected to the Atlantic Ocean by narrow passages [50]. Hence, the mean storm wave base during Serravallian-Tortonian times can be reasonably assumed at 20 m below sea level (mbsl) and the exceptional storm wave base at 30 mbsl, both marking the slope break that separates infralittoral and littoral depositional settings from offshore deposition.

Subunits 2, 3, and 4 are separated by sedimentary successions in which silt grain size is minor and clay grain size is absent. These successions contain a variety of shallow-water marine fossils (bryozoan, echinoderms, bivalves, and coralline algae) and have low-angle cross stratification, rounded cobbles and pebbles and other evidence of above wave base settings as shown above. Therefore, the sedimentary units separating the volcanic subunits of the Los Frailes Formation can be collectively interpreted as mixed carbonate-siliciclastic platform-beach facies deposited in infralittoral to littoral settings. The fines-depleted character, soft-sediment deformation structures, low-angle cross-bedding and interbedding with sedimentary rocks from shallow-water settings suggest subaqueous deposition of volcanic subunit 3 of the Los Frailes Formation [8]. Hence, the composite stratigraphic succession obtained from lateral correlation in the Los Frailes area includes thin sedimentary units deposited in infralittoral to littoral settings (0–20 mbsl) and thicker volcanic units emplaced in deeper, likely offshore, settings (>20 mbsl). Based on these paleobathymetyric constraints, the relative sea-level curve can be obtained with hiatuses corresponding to the unconformities at the contacts between volcanic and sedimentary units (**Figure 15**). Fluidization of unconsolidated sediments into overlying lavas suggests that the time encompassed from deposition of sediments to lava emplacement was not very long. Based on the ages of volcanic subunits and on the number of volcanic subunits of the Los Frailes formation, the periodicity of volcanic cycles can be roughly approximated at 10^5 years. Volcanic activity during each volcanic cycle includes constructive and destructive events of volcanic edifices and is assumed to have occurred in a relatively short time span ($<10^4$ years). The Los Frailes area can be regarded as a volcanic field composed of individual, partly overlapping, domes that are active along a time span of about 5×10^5 years with periods of volcanic repose separating dome activity. A similar scenario has been proposed for Surtseyan volcanism of the Eocene-Oligocene Waiareka-Deborah volcanic field in New Zealand but encompassing a time span of several 10^6 years [51]. The accumulated thickness of the stratigraphic succession at Los Frailes is mainly derived from the volcanic activity while the sedimentary succession accumulated during repose periods has much smaller thickness (**Figure 15**). Sea-level oscillations can be explained by the progradation and retrogradation of mixed carbonate-siliciclastic platform-beach wedges after each volcanic cycle and by infilling of offshore settings with volcanic material during volcanic cycles. This

dynamics requires tectonic subsidence to accommodate the thickness of volcanic material accumulated during volcanic cycles in infralittoral to littoral sediments. Similar to other Neogene basins of the Betic-Rif Orogen [52–54], we propose that tectonic subsidence in Cabo de Gata is controlled by uplift-downdrop displacements along major strike-slip faults that bound the Almeria-Níjar basin (i.e., the Carboneras fault) and/or by vertical displacements along minor faults associated with these major faults.

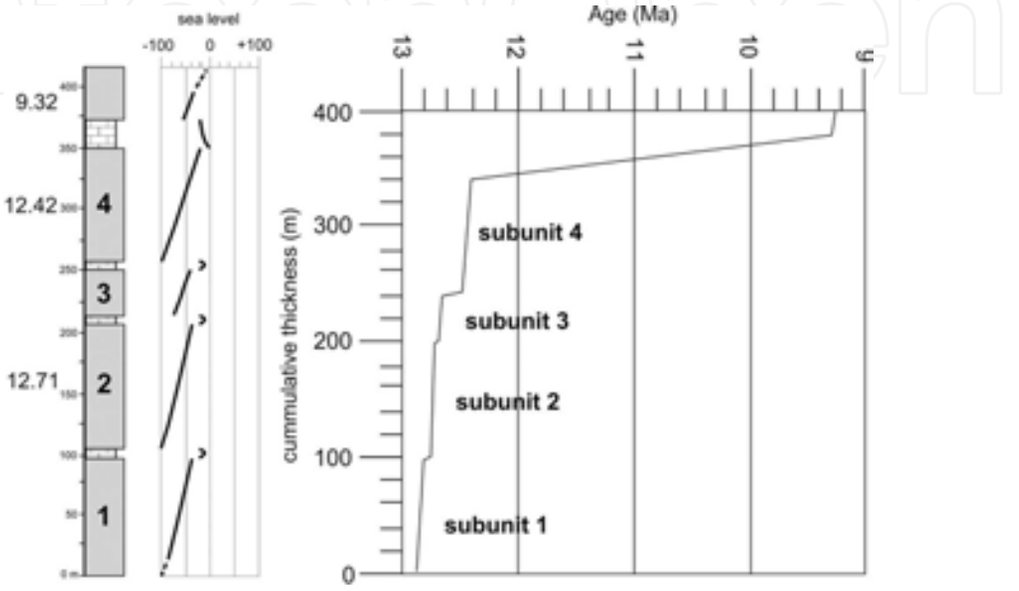

Figure 15. Composite stratigraphic log of the Los Frailes area based on the lateral correlation of **Figure 13** with sea-level curve based on the bathymetric constrains from sedimentary units and volcanic units (1–4) and cumulative thickness versus age.

8. Conclusion

Volcanism in Cabo de Gata is cyclic, with eruptive periods being characterized by both construction and partial dismantling of volcanic edifices, whereas noneruptive periods are characterized by volcanic repose, sedimentation of carbonate and siliciclastic rocks and erosion of volcanic edifices and deposits. The El Barronal Formation, the Los Frailes Formation and many other units in Cabo de Gata, which are divided into volcanic subunits separated by sedimentary units, are the geological record of this cyclic volcanism and volcanic hiatus history. Volcanic activity in Cabo de Gata includes effusive and explosive eruptions and syn-eruptive partial collapse of volcanic edifices yielding avalanches of volcanic debris deposited in submarine settings. The characteristic eruption model in Cabo de Gata likely began with explosive eruptions that produced juvenile and lithic fragments and deposition of pyroclastic density currents and ended with the effusion of lavas. Volcanic debris-avalanche deposits of the Los Frailes Formation and the Cerro Estorvillas Formation resulted from the sector collapse of submarine to emergent lava domes and were deposited in offshore settings. They constitute rare examples in the geological record of submarine volcanic debris avalanches that can be

http://dx.doi.org/10.5772/63579

studied by direct access on exposed outcrops. Based on depositional setting of sedimentary rocks and on thickness and ages of volcanic rocks, it is suggested that the volcanic pile produced during each volcanic cycle in infralittoral to littoral settings is accommodated by tectonic subsidence along major faults controlling the Almeria-Níjar basin.

Acknowledgements

We thank Miguel Garcés for comments and suggestions on a first version of the manuscript. This research has been partly funded by project 2014SGR1595 and by grant PRX14/00303 to Carles Soriano.

Author details

Carles Soriano[1*], Ray A.F. Cas[2*], Nancy R. Riggs[3*] and Guido Giordano[4*]

*Address all correspondence to: csoriano@ictja.csic.es, ray.cas@nau.edu, nancy.riggs@nau.edu and guido.giordano@uniroma3.it

1 Institute of Earth Sciences "Jaume Almera", Superior Council for Scientific Research c/ Lluís Solé Sabarís s/n, Barcelona, Spain

2 School of Earth, Atmosphere and Environment, Monash University, Monash University, Calyton Campus, Australia

3 Geology Program, School of Earth Sciences and Environmental Sustainability, Northern Arizona University, Flagstaff, USA

4 Department of Science, Geological Sciences Section, Roma Tre University, Largo S. Leonardo Murialdo, Roma, Italy

References

[1] Fuster JM, Aguilar MJ, García A. Las sucesiones volcánicas en la zona del Pozo de los Frailes dentro del vulcanismo cenozoico del Cabo de Gata (Almería). Estudios Geológicos. 1965; XXI: 199–222.

[2] Páez Carrión A, Sánchez Soria P. Vulcanología del Cabo de Gata, entre San José y Vela Blanca. Estudios Geológicos. 1965; XXI: 223–246.

[3] León C. Las formaciones volcánicas del Cerro de los Lobos (Almería, SE. de España). Estudios Geológicos. 1967; XXIII: 15–28.

[4] Di Battistini G, Toscani L, Iaccarino S, Villa IM. K/Ar ages and the geological setting of calc-alkaline volcanic rocks from Sierra de Gata, SE Spain. Neues Jahrbuch für Mineralogie, Monatshefte. 1987; H 8: 369–383.

[5] Cunningham CG, Arribas A Jr, Rytuba JJ, Arribas A. Mineralized and unmineralized calderas in Spain; Part 1, evolution of the Los Frailes caldera. Mineralium Deposita 1990; v. 25 (supp.): S21–S28.

[6] Arribas A Jr, Cunningham CG, Rytuba JJ, Rye RO, Kelly WC, Podwysocki MH, McKee EH, Tosdal RM. Geology, Geochronology, Fluid inclusions, and Isotope Geochemistry of the Rodalquilar Gold Alunite Deposit Spain. Economic Geology.1995; 90: 795–822.

[7] Cas RAF, Giordano G. Submarine volcanism: a review of the constrains, processes and products and relevance to the Cabo de Gata volcanic succession. Italian Journal of Geosciences. 2014; 133: 362–377.

[8] Soriano C, Riggs N, Giordano G, Porreca M, Conticelli S. Cyclic growth and mass wasting of submarine Los Frailes lava flow and dome complex in Cabo de Gata, SE Spain. Journal of Volcanology and Geothermal Research. 2012; 231–232: 72–86.

[9] Soriano C, Giordano G, Cas R, Riggs N, Porreca M. Facies architecture, emplacement mechanisms and eruption style of the submarine andesite El Barronal complex, Cabo de Gata, SE Spain. Journal of Volcanology and Geothermal Research. 2013; 264: 210–222.

[10] Soriano C, Giordano G, Riggs N, Porreca M, Bonamico A, Iosimi D, Cifelli F, Mattei M, De Benedetti A, Guarnieri L, Marchionni S. Geologic map, volcanic stratigraphy and structure of the Cabo de Gata volcanic zone, Betic-Rif Orogen, SE Spain. Italian Journal of Geosciences. 2014; 133: 325–340.

[11] Porreca M, Cifelli F, Soriano C, Giordano G, Romano C, Conticelli S, Mattei M. Hyaloclastite fragmentation below the glass transition: an example from El Barronal submarine volcanic complex (Spain). Geology. 2014; 42: 87–90.

[12] Porreca M, Cifelli F, Soriano C, Giordano G, Mattei M. Magma flow within dykes in submarine hyaloclastite environments: an AMS study of the Miocene Cabo de Gata volcanic units. In: Ort MH, Porreca M, Geissman JW, editors. The Use of Palaeomagnetism and Rock Magnetism to Understand Volcanic Processes. Geological Society, London, Special Publication, 396; 2015. p. 133–157.

[13] van Otterloo J, Cas RAF, Scutter C. The fracture behaviour of volcanic glass and relevance to quench fragmentation during formation of hyaloclastite and phreatomagmatism. Earth Science Reviews. 2015; 151: 79–116.

[14] Sharqawy M, Lienhard JH, Zubair SM. Thermophysical properties of seawater: a review of existing correlations and data. Desalination and water treatment. 2010; 16: 354–380.

[15] Höskuldsson A, Sparks RSJ. Thermodynamics and fluid dynamics of effusive subglacial eruptions. Bulletin of Volcanology. 1997; 59: 219–230.

[16] Zimanowski B, Buttner R. Phreatomagmatic explosions in subaqueous volcanism. In: White JDL, Smellie JL, Clague DA, editors. Submarine Explosive Volcanism. American Geophysical Union, Monograph, 140; 2003. pp. 51–60.

[17] Wohletz KH. Water/magma interaction: physical considerations for the deep submarine environment. In: White JDL, Smellie JL, Clague DA, editors. Submarine Explosive Volcanism. American Geophysical Union, Monograph, 140; 2003. pp. 25–49.

[18] Doblas M, López-Ruiz J, Cebriá JM. Cenozoic evolution of the Alboran Domain: a review of the tectonomagmatic models. In: Beccaluva L, Bianchini G, Wilson M, editors Cenozoic Volcanism in the Mediterranean area. Geological Society of America, Special Paper, 418; 2007. pp. 303–320.

[19] Lustrino M, Duggen S, Rosenberg C. The central-western Mediterranean: anomalous igneous activity in an anomalous collisional tectonic setting. Earth Science Reviews. 2011; 104: 1–40.

[20] Vergés J, Fernàndez M. Tethys-Atlantic interaction along the Iberia-Africa plate boundary: The Betic-Rif orogenic system. Tectonophysics. 2012; 579: 144–172.

[21] Conticelli S, Guarnieri L, Farinelli A, Mattei M, Avanzinelli R, Bianchini G, Boari E, Tommasini S, Tiepolo M, Prelevic D, Venturelli G. Trace elements and Sr-Nd-Pb isotopes of K-rich, shoshonitic, and calc-alkaline magmatism of the Western Mediterranean Region: genesis of ultrapotassic to calc-alkaline magmatic associations in a post-collisional geodynamic setting. Lithos. 2009; 107: 68–92.

[22] Mattei M, Riggs N, Conticelli S, Giordano G, Cifelli F, Soriano C, Jicha B, Marchionni S, Guarnieri L, Tommasini S, Jasim A, Franciosi L, Porreca M. Geochronology geochemistry and geodynamics of the Cabo de Gata volcanic zone, South Eastern Spain. Italian Journal of Geosciences. 2014; 133: 341–361.

[23] Faccenna C, Piromallo C, Crespo-Blanc A, Jolivet L, Rossetti F. Lateral slab deformation and the origin of the western Mediterranean arcs. Tectonics. 2004; 23: TC1012.

[24] Comas MC, Platt JP, Soto JI, Watts AB. The origin and tectonic history of the Alboran basin; insights from Leg 161 results. In: Zahn R, Comas MC, Klaus A, editors. Proceedings of the Ocean Drilling Program, Scientific Results, 161; 1999. pp. 555–580.

[25] McClusky HL, Conner ME, Smith LD, Holloway MV, Conover TA, Beasley DE. Mapping of the lateral flow field in typical subchannels of a support grid with vanes. Journal of Fluids Engineering. 2003; 125(6): 987–996.

[26] Iribarren L, Verges J, Camurri F, Fullea J, Fernandez M. The structure of the Atlantic–Mediterranean transition zone from the Alboran Sea to the Horseshoe Abyssal Plain (Iberia-Africa plate boundary). Marine Geology. 2007; 243: 97–119.

[27] Bell JW, Amelung F, King GCP. Preliminary late quaternary slip history of the Carboneras fault, Southeastern Spain. Journal of Geodynamics. 1997; 24: 51–66.

[28] Scotney P, Burgess R, Rutter EH. 40Ar/39Ar age of the Cabo de Gata volcanic series and displacements on the Carboneras fault zone, SE Spain. Journal of the Geological Society, London. 2000; 157: 1003–1008.

[29] Rutter EH, Burgess R, Faulkner DR. Constraints on the movement history of the Carboneras Fault Zone (SE Spain) from stratigraphy and ^{40}Ar-^{39}Ar dating of Neogene volcanic rocks. In: Llana-Fúnez S, Marcos A, Bastida F, editors. Deformation Structures and Processes within the Continental Crust. Geological Society, London, Special Publications, 394; 2014. pp. 79–99.

[30] Pedrera A, Marín-Lechado C, Galindo-Zaldívar J, Rodríguez-Fernández LR, Ruiz-Constán A. Fault and fold interaction during development of the Neogene-Quaternary Almería-Níjar basin (SE Betic Cordilleras). In: Moratti G, Chalouan A, editors Tectonics of the Western Mediterranean and North Africa. Geological Society, London, Special Publication, 262; 2006. pp. 217–230.

[31] Borehole dataset of the Instituto Geologico y Minero of Spain. Available from www.igme.es

[32] Brachert TC, Hultzsch N, Knoerich AC, Krautworst UMR, Stückrad OM. Climatic signature in shallow-water carbonates: high-resolution stratigraphic markers in carbonate build-ups (Late Miocene, southern Spain). Palaeogeography, Palaeoclimatology, Palaeoecology. 2001; 175: 211–237.

[33] Ballesteros M, Rivera J, Muñoz A, Muñoz-Martín A, Acosta J, Carbo A, Uchupi E. Aboran basin southern Spain-Part II. Neogen tectonic implications for the orogenic float model. Marine and Petroleum Geology. 2008; 25: 75–101.

[34] (IGME) Instituto Geológico y Minero de España. Mapa Geológico de España 1:50000, El Pozo de los Frailes 1060. Servicio de Publicaciones del Ministerio de Industria y Energía, Madrid. 1983.

[35] Duggen S, Hoernle K, van den Bogaard P, Harris C. Magmatic evolution of the Alboran region: The role of subduction in forming the western Mediterranean and causing the Messinian Salinity Crisis. Earth and Planetary Science Letters. 2004; 218: 91–108.

[36] Montgomery P, Farr MR, Franseen EK, Goldstein RH. Constraining controls of carbonate sequences with high-resolution chronostratigraphy: Upper Miocene, Cabo de Gata region, SE Spain. Palaeogeography, Palaeoclimatology, Palaeoecology. 2001; 176: 11–45.

[37] Trofimovs J, Cas RAF, Davis BK. An Archean submarine volcanic debris avalanche deposit, Yilgarn Craton, western Australia, with komatiite, basalt and dacite megablocks. The product of dome collapse. Journal of Volcanology and Geothermal Research. 2004; 138: 111–126.

[38] Crandell DR, Miller CD, Glicken HX, Christiansen RL, Newhall CG. Catastrophic debris avalanche from ancestral Mount Sashta, California. Geology. 1984; 12: 143–146.

[39] Glicken HX. Sedimentary architecture of large volcanic-debris avalanches. In: Smith GA., Fisher RV, editors. Sedimentation in volcanic settings. SEPM Tulsa Special Publication, 45; 1991. pp. 99–106.

[40] Palmer BA, Alloway BV, Neall VE. Volcanic-debris-avalanche deposits in New Zealand-Lithofacies organization in unconfined, wet-avalanche flows. In: Smith GA., Fisher RV, editors. Sedimentation in Volcanic settings. SEPM Tulsa Special Publication, 45; 1991. pp. 89–98.

[41] Stoopes GR, Sheridan MF. Giant debris avalanche from the Colima Volcanic Complex, México, implications for long runout landslides (<100°km) and hazard assessment. Geology. 1992; 20: 299–302.

[42] Roverato M, Cronin S, Procter J, Capra L. Textural features as indicators of debris avalanche transport and emplacement, Taranaki volcano. Geological Society of America bulletin. 2014. DOI:10.1130/B30946.1.

[43] Voight B, Komorowski JC, Belusov AB, Belusova M, Boudon G, Francis PW, Franz V, Heinrich P, Sparks RSJ, Young SR. The 26 December (Boxing Day) 1997 sector collapse and debris avalanche at Soufrière Hills Volcano, Montserrat. In: Druitt TH, Kokelaar BP editors. The eruption of Soufrière Hills Volcano, Montserrat, from 1995–1999. Geological Society London Memoir 21; 2002. pp. 363–407.

[44] Siebert L. Large volcanic debris avalanche: characteristics of source areas, deposits and associated eruptions. Journal of Volcanology and Geothermal Research. 1984; 22: 163–197.

[45] Ui T, Glicken HX. Internal structural characteristics of debris avalanche from Mount Sahsta, California, U.S.A. Bulletin of Volcanology. 1986; 48: 189–194.

[46] Flügel E. Microfacies of Carbonate Rocks. Springer Berlin Heidelberg; 2004. 976 p.

[47] Brandano M, Ronca S. Depositional processes of the mixed carbonate-siliciclastic rhodolith beds of the Miocene Saint-Florent Basin, northern Corsica. Facies. 2014; 60: 73–90.

[48] Nalin R, Nelson CS, Basso D, Massari F. Rhodolith-bearing limestones as transgressive marker beds: fossil and modern examples from North Island, New Zealand. Sedimentology. 2008; 55: 249–274.

[49] Hernández-Molina FJ, Fernández-Salas LM, Lobo F, Somoza L, Díaz-del-Río V, Alveirinho Dias JM. The infralittoral prograding wedge: a new large-scale progradational sedimentary body in shallow marine environments. Geo-Marine Letters. 2000; 20: 109–117.

[50] Martín JM, Braga JC, Aguirre J, Puga-Bernabéu A. History and evolution of the North-Betic Strait (Prebetic Zone, Betic Cordillera): A narrow, early Tortonian, tidal-domi-

nated, Atlantic-Mediterranean marine passage. Sedimentary Geology. 2009; 216: 80–90.

[51] Moorhouse BL, White JDL, Scott, J. Cape Wanbrow: A stack of Surtseyan-style volcanoes built over millions of years in the Waiareka-Deborah volcanic field, New Zealand. Journal of Volcanology and Geothermal Research. 2015; 298: 27–46.

[52] Soria J, Viseras C, Fernández J. Late Miocene-Pleistocene tectono-sedimentary evolution and subsidence history of the central Betic Cordillera (Spain): a case study of the Guadix intramontane basin. Geological Magazine. 1998; 135: 565–574.

[53] Garcés M, Krijgsman W, Agustí J. Chronostratigraphic framework and evolution of the Fortuna basin (Eastern Betics) since the Late Miocene. Basin Research. 2001; 13: 199–216.

[54] Rodríguez-Fernández J, Sanz de Galdeano C. Late orogenic intramontane basin development: the Granada basin, Betics (southern Spain). Basin Research. 2006; 18: 85–102.